remote sensing

MDPI

Article

Is It Reliable to Extract Gully Morphology Parameters Based on High-Resolution Stereo Images? A Case of Gully in a "Soil-Rock Dual Structure Area"

Tingting Yan [1], Weijun Zhao [1,*], Fujin Xu [2], Shengxiang Shi [1], Wei Qin [3], Guanghe Zhang [4] and Ningning Fang [5]

[1] School of Civil Engineering and Geomatics, Shandong University of Technology, Zibo 255000, China; yanting@sdut.edu.cn (T.Y.); 21110905002@stumail.sdut.edu.cn (S.S.)
[2] College of Geography and Remote Sensing Sciences, Xinjiang University, Urumqi 830046, China; xfj@stu.xju.edu.cn
[3] State Key Laboratory of Simulation and Regulation of Water Cycle in River Basin, China Institute of Water Resources and Hydropower Research, Beijing 100048, China; qinwei@iwhr.com
[4] School of Ecology and Environment, Southwest Forestry University, Kunming 650224, China; zgh0406@swfu.edu.cn
[5] Ecological Environment Monitoring Center of Zibo, Zibo 255000, China; zhangjingjing@zb.shandong.cn
* Correspondence: zhaoweijun@sdut.edu.cn

Abstract: The gully morphology parameter is an important quantitative index for monitoring gully erosion development. Its extraction method and accuracy evaluation in the "soil-rock dual structure area" are of great significance to the evaluation of gully erosion in this type of area. In this study, unmanned aerial vehicle (UAV) tilt photography data were used to evaluate the accuracy of extracting gully morphology parameters from high-resolution remote sensing stereoscopic images. The images data (0.03 m) were taken as the reference in Zhangmazhuang and Jinzhongyu small river valleys in Yishui County, Shandong Province, China. The accuracy of gully morphology parameters were extracted from simultaneous high-resolution remote sensing stereo images data (0.5 m) was evaluated, and the parameter correction model was constructed. The results showed that (1) the average relative errors of circumference (P), area (A), linear length of bottom (L1), and curve length of bottom (L2) are mainly concentrated within 10%, and the average relative errors of top width (TW) are mainly within 20%. (2) The average relative error of three-dimensional (3D) parameters such as gully volume (V) and gully depth (D) is mainly less than 50%. (3) The larger the size of the gully, the smaller the 3D parameters extracted by visual interpreters, especially the absolute value of the mean relative error (R_{mean}) of V and D. (4) A relationship model was built between the V and D values obtained by the two methods. When V and D were extracted from high-resolution remote sensing stereo images, the relationship model was used to correct the measured parameter values. These findings showed that high-resolution remote sensing stereo images represents an efficient and convenient data source for monitoring gully erosion in a small watershed in a "soil-rock dual structure area".

Keywords: gully morphology; accuracy assessment; UAV; high-resolution remote sensing stereo image; soil-rock dual structure area

Citation: Yan, T.; Zhao, W.; Xu, F.; Shi, S.; Qin, W.; Zhang, G.; Fang, N. Is It Reliable to Extract Gully Morphology Parameters Based on High-Resolution Stereo Images? A Case of Gully in a "Soil-Rock Dual Structure Area". *Remote Sens.* **2024**, *16*, 3500. https://doi.org/10.3390/rs16183500

Academic Editor: Takashi Oguchi

Received: 13 July 2024
Revised: 13 September 2024
Accepted: 16 September 2024
Published: 21 September 2024

1. Introduction

Soil erosion has become one of the serious ecological and environmental problems faced by all mankind [1–3]. Gully is one of the main types of gully erosion and is a result of soil erosion [4,5]. The gully head generally develops on a larger slope, while the gully tail cuts into the valley floor, and its size increases with an increase in the flow and slope [6]. A gully is characterized by a large amount of erosion and a high erosion rate. It destroys land resources and farmland, affecting grain production and ecological balance [7,8]. It is also an important source of sediments in the basin [9–11]. However, owing to the complexity of gully development and morphology [9–11], monitoring its

temporal and spatial evolution becomes challenging, thus hindering the understanding of gully erosion mechanism [11–14]. Studies monitoring the gully morphology evolution in the Yimeng Mountain area of China with a typical "soil-rock dual structure" are scarce [15–17]. Therefore, it is necessary to use appropriate monitoring methods to obtain long-term gully morphology parameters and monitor gully development to explore its erosion mechanism, development law, quantitative simulation, and influencing factors [11,15–17].

In recent years, remote sensing technologies, such as high-resolution remote sensing images, aerial photography, laser radar (LiDAR), three-dimensional (3D) laser scanning [18–23], three-dimensional photo reconstruction and oblique photogrammetry [24], field measurement [25], and other comprehensive methods [26–32], have been used to monitor groove erosion. Among them, high-resolution remote sensing images are superior to other traditional measurement methods in terms of accuracy and effectiveness, thus providing relatively accessible and reliable data [17,18]. They provide multi-source data for gully morphology parameters, such as width, length, perimeter, and area, representing an important data source for monitoring gully erosion. Thus, they allow large-scale monitoring of gully morphology [11,17–19]. However, they are rarely used in the Yimeng Mountain area where gullies are abundant [17,20].

3D laser scanning total station, with its characteristics of non-contact and penetration, can obtain high-precision terrain data efficiently and quickly [18,19,21–23]. These features save a lot of manpower and financial resources and have significant advantages. However, it is limited by issues such as scanning dead corners, cumbersome data processing, and unsuitability for large-scale monitoring. In addition, with its rapid development, UAV remote sensing technology has been widely used in mapping, soil and water conservation research, and other fields [33–35]. UAV tilt photogrammetry technology can address the space limitation of ground-based laser scanning technology to a certain extent and line of sight occlusion caused by traditional UAV aerial photography [36]. Moreover, high-resolution (centimeter-level) orthophoto images and elevation data can be obtained from UAV tilt photogrammetry using professional software [27,35]. This technique provides a scientific and advanced method for monitoring the shape characteristics of the gully in a "soil-rock dual structure" area. However, compared with remote sensing images, it is only suitable for monitoring gully erosion on a small scale because of the time consuming. In addition, to ensure flight safety and the accuracy of data acquisition, the collection and processing processes should be completed by experienced professional pilots and professionals using professional software [37]. Extracting the morphology parameters of gullies based on high-resolution remote sensing stereo image data can address the shortcomings of the above research methods. An accuracy analysis of DEM extraction based on high-resolution remote sensing stereo images has been previously performed [38,39]. Thus, the accuracy of extracting gully morphology parameters based on high-resolution remote sensing stereo image data to monitor gully development in a "soil-rock dual structure" area remains unclear, which limits the application of this new technology.

This study aims to determine the accuracy of extracting gully morphology parameters in a "soil-rock dual structure" area based on high-resolution remote sensing stereoscopic image data. A correction model was built with UAV oblique photography data, so as to obtain gully morphology parameters in the mesoscale region of the "soil-rock dual structure" area conveniently, quickly and accurately. Therefore, this study takes two small watersheds (ZhangMazhuang and Jinzhongyu, Shagou Town, Yishui County, Shandong Province, China) as examples. The accuracy of the gully morphology parameters extracted from high-resolution satellite remote sensing stereo image data was calculated, and the error range of morphological parameters was determined. The causes of error were analyzed, and the solutions to minimize them were discussed. This study presents a more scientific and advanced method for monitoring gully erosion and its formation mechanism in the mesoscale area of a "soil-rock dual structure" area.

2. Materials and Methods

2.1. Study Area

The Zhangmazhuang and Jinzhongyu small watersheds located in Shagou Town, Yimeng Mountain area were selected as examples. This is a typical "soil-rock dual structure" area [17,40], with high soil erodibility and extensive development of gully (36°06′04″N~36°08′57″N, 118°38′01″E~118°39′59″E, Figure 1). It covers an area of approximately 16 km^2. The annual average temperature is 12–14 °C, and the annual average precipitation is 830 mm; thus, it belongs to a warm temperate monsoon climate region. In the study area, the soil contains more gravel, soil layer is thin, vegetation coverage is low, biodiversity is single, soil erosion is serious, and gully development is extensive. Owing to an increase in sloping cropland and changing land use behavior, such as indiscriminate land reclamation, gully erosion has intensified in this area. The main land use types are cropland, wasteland, and woodland.

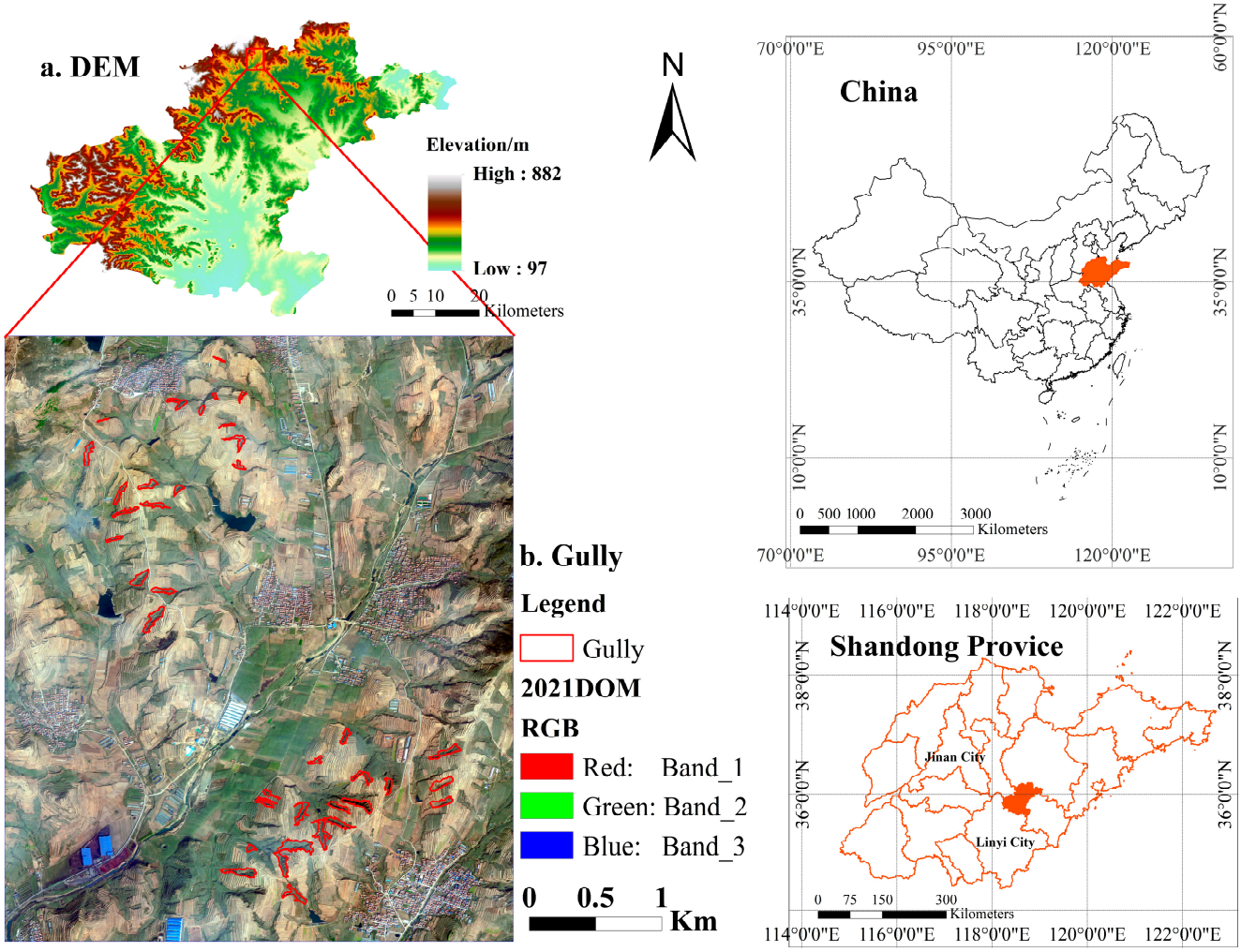

Figure 1. Location map of the study area. Note: Figure (**a**) is the DEM map of Yishui County; Figure (**b**) is the enlarged map of the study area and gully distribution; the two maps on the right are the zoning maps of China and Shandong Province.

2.2. Methods

2.2.1. Technical Flow

Gully parameters extraction and precision analysis were performed in three parts: extraction of gully morphological parameters based on UAV and high-resolution remote sensing stereo images, accuracy analysis of gully morphological parameters based on high-resolution remote sensing stereo images, and error source analysis (Figure 2).

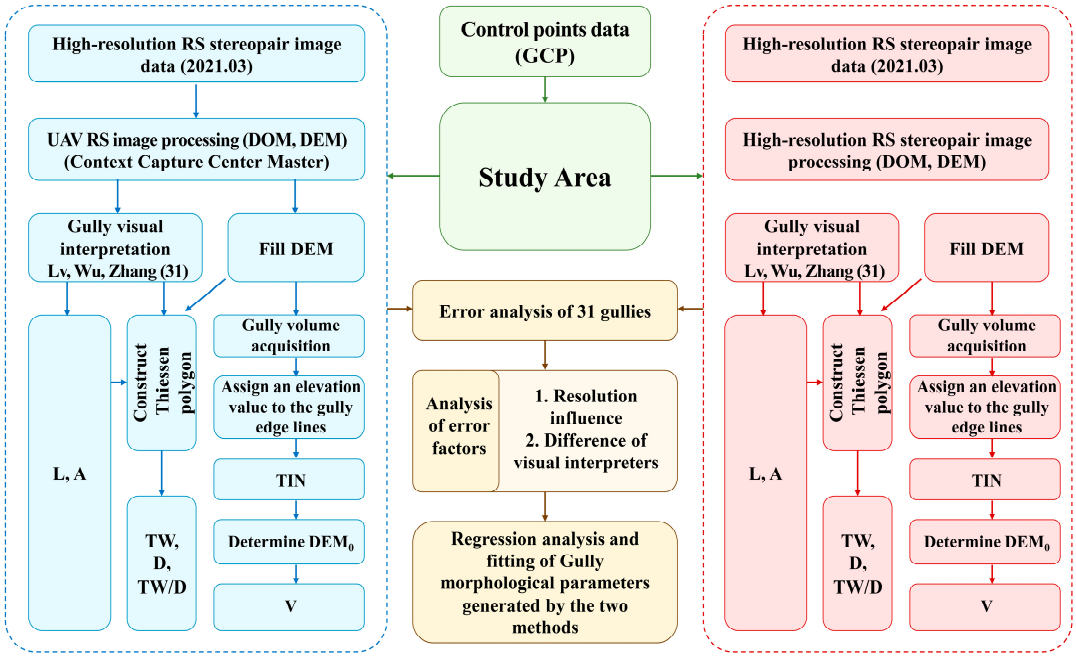

Figure 2. Technical flow chart.

2.2.2. UAV Tilt Photography Measurement Data Acquisition and Processing

(1) Tilt photogrammetry data of UAV

The multi-rotor UAV of DJI Jingwei M600Pro (DJI Matrice600 Professional, Shenzhen, China) was used in this study, and the parameters of the UAV platform and onboard sensor are summarized in Table 1.

Table 1. The parameters of the UAV platform and onboard sensor.

UAV	Sensor	Sensor Size (mm)	Focal Length (m)	Resolution (cm)	Shooting Interval(s)
DJI M600Pro	FAST-X1 (Five-lens camera)	23.5	35 mm × 5	3 cm	2.5 s

Image data and coordinate data were collected from 31 gullies in the small watershed in 21–23 March 2021. During this period, the weather was cloudless and full of light, and the wind was less than level 4, which was completely suitable for UAV flight. The flight took 12,678 sets of photos. The relative flight altitude was 150 m, the front overlap was 80%, and the side overlap rate was 75%, so as to avoid the insufficient overlap between the images, which affects photo reconstruction.

(2) Layout of ground control points

A total of 15 ground control points were uniformly laid with red marker paint in the locations with obvious features. The size of the control points was 5–10 times higher than the image resolution. The RTK equipment was used to measure the coordinates of the control points for geometric correction of the image.

(3) Three-dimensional model and digital orthophoto map (DOM) data processing

UAV aerial data, coordinate information, and aerial triangulation data were imported. Then, adjustment of control points was carried out. Finally, a 3D model of the gully was constructed. The modeling software Context Capture 10.20, (Bentley, Exton, PA, USA), was used for the 3D modeling of erosion gully. The software can efficiently and easily generate 3D models for various types of infrastructure projects. Digital surface model (DSM) and DOM can also be produced from 3D model results.

All layer data were adopted using the Transverse Mercator projection and the WGS _1984_UTM_Zone_50N coordinate system.

2.2.3. Preprocesses of High-Resolution Remote Sensing Stereopair Image and DEM Extraction High Resolution

To ensure the synchronization, stereopair images with a spatial resolution of 0.5 m were selected, and the shooting time was scheduled on 12 February 2021. In this period, no leafy plants were growing, except for some evergreen trees such as pine in this study area. The vegetation coverage rate of the study area was 0.05, which improved the accuracy of DEM extraction from high-resolution remote sensing stereopair images.

The high-resolution remote sensing stereopair image (Worldview-3 (OR2A, 0.5 × 0.5 m), 12 February 2021) included satellite panchromatic data, a base map, elevation data, and multi-band satellite data. Pre-processing included the following steps. First, in the PCI geographic imaging accelerator software, data from ground control points (n = 15) were used for geometric correction. Then, the image was fused using the pan-sharpening method, and orthographic correction was performed. Finally, the image was homogenized, mosaiced, and cropped in Photoshop, yielding a complete DOM (0.5 × 0.5 m). PixeGrid software (v2.183) was used for three-space encryption to produce a DEM based on high-resolution remote sensing stereo images. Three-dimensional image pairs were generated based on image direction and kernel line generation, and a regional digital elevation model was established by algorithm matching. Finally, a DEM (0.5 × 0.5 m) was generated by interactive editing, embedding, and cropping.

2.2.4. Extraction of Gully Morphology Parameters

The vector boundaries along 31 gullies in the study area were visually interpreted and mapped based on the DOM generated by the tilt photogrammetry data of the UAV and high-resolution remote sensing stereopair image. The perimeter (P) and area (A) of the gully were calculated based on the GIS platform. Based on the vector boundary and DEM along 31 gullies, the linear length from the gully head to the gully mouth (L1) and the bottom curve length (L2) from the gully head to the gully mouth along the bottom line were calculated. Then, the gully volume was calculated [17–19,29]. Based on the GIS platform, the gully volume was calculated by DEM and DEM0 (original eroded surface of the gully), and the subtraction is gully volume (V).

To calculate the DEM0, the layers of the boundary of the 31 gullies were converted into point layers, and elevation values were to the point layers assigned to obtain the elevation coordinates. Based on the triangulation irregular network, the DEM was constructed according to the elevation points of 31 gullies, and the DEM0 was obtained by clipping the layers along the 31 gullies.

Finally, the section parameters of the gully were calculated to determine the section of the gully. Using the ArcGIS software (v10.8.2) and based on the curve length of the gully bottom (L2), the Tyson polygon method was used to determine several sections, and the gully profile was generated using the gully DEM data (Figure 3). The width, depth, and width-to-depth ratio of each section and their respective averages were determined.

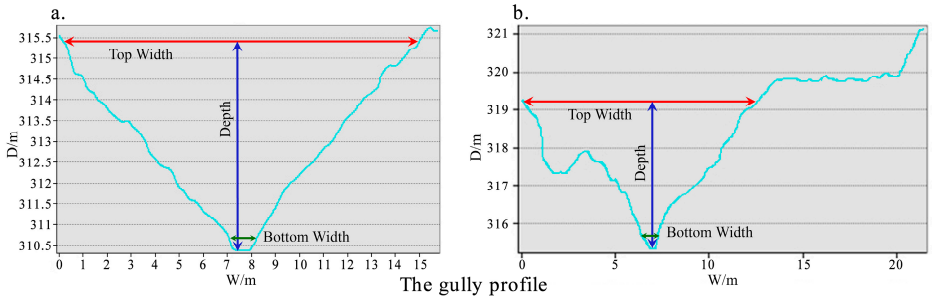

Figure 3. The width and depth cutaway view. Note: (**a**,**b**) represent different extraction methods of gully morphology parameters.

2.2.5. Error Evaluation Index

The obtained gully morphology parameter values may have errors due to differences in the visual interpretation by personnel. Therefore, several commonly used error evaluation indexes were selected to reveal the errors of gully morphology parameters extracted by high-resolution remote sensing stereo images and the errors of gully morphology parameters interpreted by different visual interpreters.

$$R_{mean\ i} = \frac{1}{n}\sum_{j=1}^{n}\left|\frac{Zij - Mi}{Mi}\right|$$

$$R_{max\ i} = max\left(\left\{\left|\frac{Zij - Mi}{Mi}\right|\right\}\right)$$

$$T_{max\ i} = max\left(\left\{|max\left(\left\{\left|\frac{Zij - Mi}{Mi}\right|\right\}\right)\right.\right.$$

where n is the number of people participating in visual interpretation (n = 3), i is the gully number, and j is the number of personnel involved in visual interpretation. Zij represents the visual interpretation result of the gully i by personnel j; Mi represents the true value of the morphology parameter of the gully numbered I; R_{mean} is the absolute value of the average relative error; R_{max} is the absolute value of the maximum relative error; and T_{max} is the maximum error of differences in the visual interpretation by personnel.

3. Results

3.1. Accuracy Analysis of Morphology Parameters Extracted from High-Resolution Stereo Images

The deviations across gully morphology parameters within the study area varied, and the results of the same gully morphology parameter values obtained by different personnel via visual interpretation differed (Figure 4). Among the one- and two-dimensional gully parameters, the R_{mean} errors of other gully morphological parameters were approximately 5%, except for that of gully width, which fluctuated at approximately 10%. Regarding 3D morphology parameters, the R_{mean} errors of gully volume and depth fluctuated at 30%, and those of the width-to-depth ratio of gullies were larger, ranging between 8.5% and 376.4%. The R_{max} error of gully perimeter (P) ranged between 2.1% and 34.1%; area, 4.5% and 43.3%; gully bottom straight line length (L1), 0.5% and 18.6%; gully bottom curved line length (L2), 1.8% and 23.1%; volume, 11.8% and 110.6%; width, 7.2% and 109.5%; depth, 7.4% and 70.6%; and width-to-depth ratio, 18.0% and 509.2%.

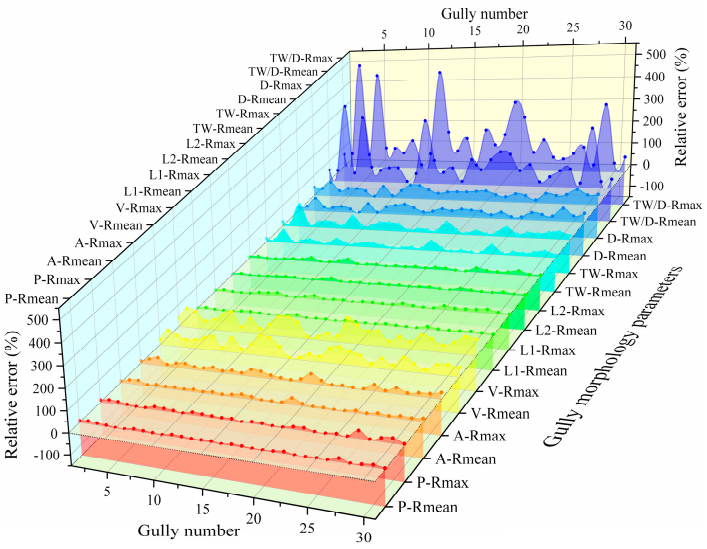

Figure 4. Relative error of gully morphology parameters extracted from high-resolution remote sensing stereo images.

The classification statistics of the R_{mean} error of gully morphology parameters obtained from high-resolution remote sensing stereo images are shown in Figure 5. Regarding one- and two-dimensional parameters, the R_{mean} errors of perimeter, area, gully bottom straight line length (L1), and gully bottom curved line length (L2) were mainly distributed within 10%, accounting for 81%, 52%, 94%, and 94% of the total sample size, respectively. The R_{mean} errors of gully width were mainly distributed within 20%, accounting for 77% of the total sample size. Regarding 3D morphology parameters, the R_{mean} errors of gully volume and depth were within 50%, accounting for 61% and 90% of the total sample size, respectively.

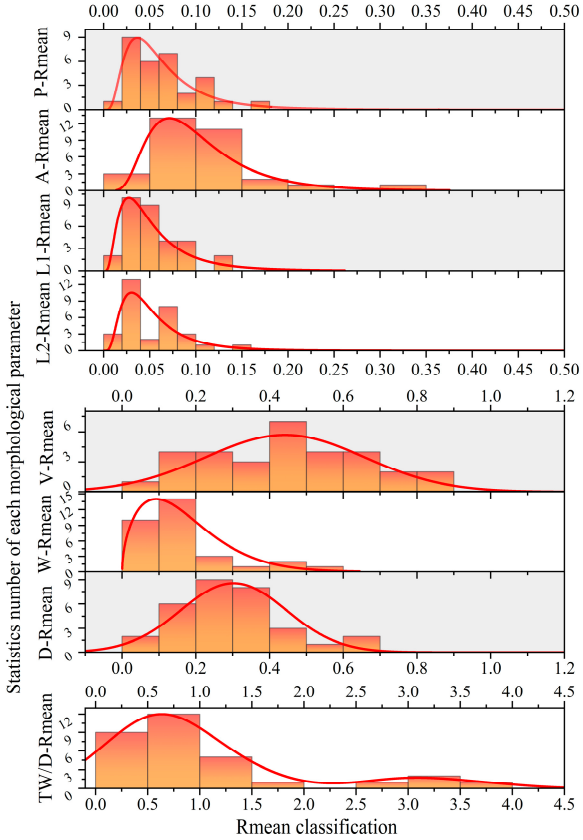

Figure 5. R_{mean} classification results of gully morphology parameter error were extracted from high-resolution remote sensing stereo images.

Overall, the extraction of one- and two-dimensional morphology parameters of gullies based on high-resolution remote sensing stereo image data was highly accurate. However, for some gullies in the study area, there was a significant error in extracting 3D morphology parameter values compared to the actual measurements.

3.2. Factors Influencing Visual Interpretation Accuracy

3.2.1. Visual Interpreters

The determination of gully morphological parameters by visual interpretation of remote sensing images is subject to various factors, including the interpreter's expertise, physiological factors, and psychological influences. Consequently, notable disparities may arise in the derived results of gully morphological parameters when different visual interpreters are involved. As shown in Figure 6, the average relative errors associated with the extraction of gully morphological parameters—such as perimeter (P), area (A), gully bottom straight line length (L1), and gully bottom curved line length (L2)—by distinct visual interpreters clustered around 10%, suggesting relatively modest errors in assessing

two-dimensional morphological parameters. Consequently, their reliability surpassed that of three-dimensional morphological parameters.

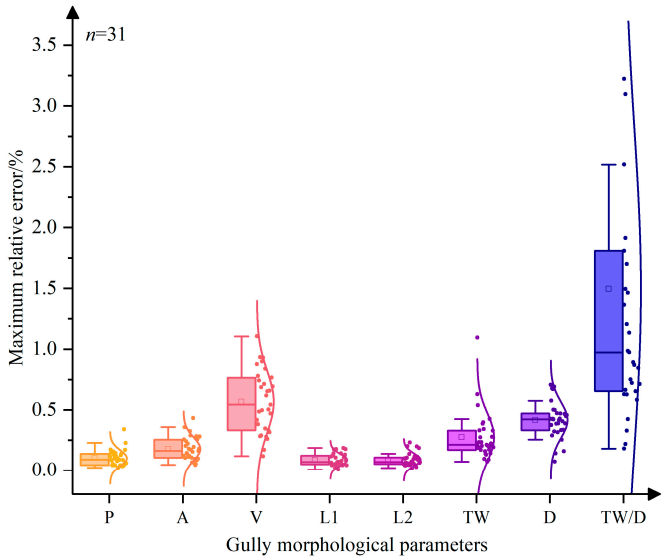

Figure 6. The maximum relative error (T_{max}) of gully morphological parameters extracted across various visual interpreters. P denotes the perimeter; A, area; L1, gully bottom straight line length; L2, gully bottom curved line length; V, volume; W, width; D, depth; W/D, width-to-depth ratio.

3.2.2. Spatial Resolution of Stereo Image

The spatial resolution of remote sensing images refers to the smallest ground unit that can be identified on the image, that is, the ground area represented by each pixel. The extraction of the DEM based on high-resolution remote sensing stereo images for calculating the three-dimensional parameters of gullies has a significant deviation. Compared to the DSM and DOM extracted from the UAV oblique photogrammetry data of the study area, the DEM and DOM from high-resolution remote sensing stereo images have a lower resolution; thus, the latter could not fully express the internal details of the gullies, as seen in Figures 7 and 8. Therefore, the depth and volume measurements of gullies calculated based on the DEM extracted from high-resolution remote sensing stereo images were generally less than their actual values, especially for smaller gullies, where the errors in 3D morphology parameters are more evident (Figure 9). Hence, this method can yield more accurate data when larger gullies are studied.

Figure 7. Interior details of the gully head (UAV image; resolution: 0.03 m).

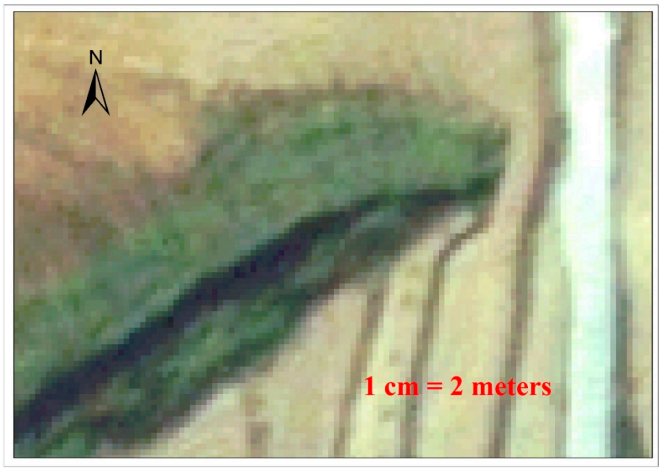

Figure 8. Internal details of the gully head (high-resolution remote sensing stereo image; resolution: 0.5 m).

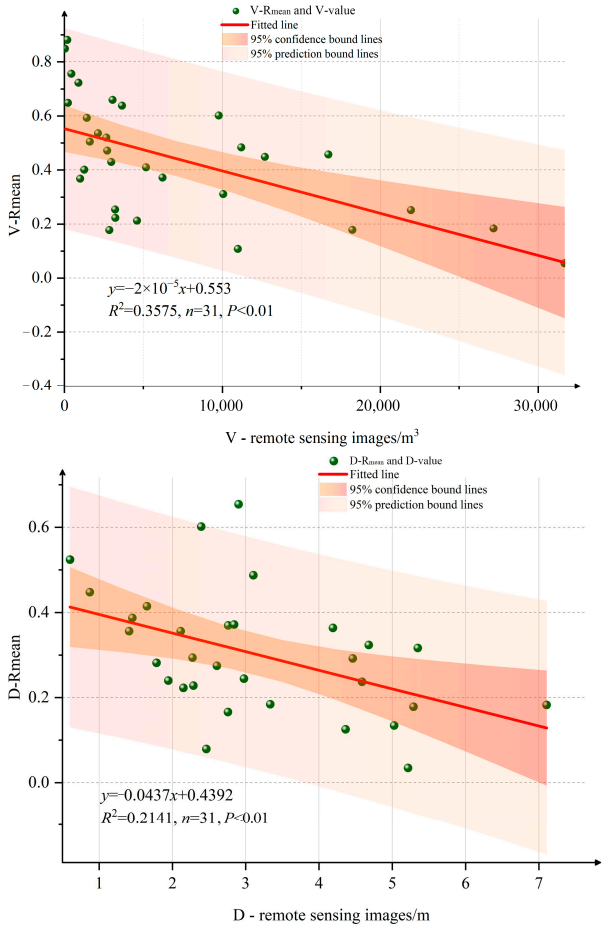

Figure 9. The relationship between the 3D morphology parameters of the gully, and the error R_{mean} was extracted based on high-resolution remote sensing stereo image.

3.3. Relationship of 3D Morphology Parameters Extracted from Oblique Photogrammetry and Remote Sensing Images

Based on the relationship between the 3D morphology parameters of gullies obtained from UAV oblique photogrammetry data and those obtained from high-resolution remote sensing stereo image data, good relationship models were established for the parameters gully volume and depth. The volume correction model is represented by $y = -3 \times 10^{-5}x^2 + 2.0251x - 69.501$ ($R^2 = 0.9297$, $p < 0.01$), and the depth correction model is represented by

$y = 1.6725x^{0.816}$ ($R^2 = 0.6504$, $p < 0.01$) (Figure 10). These relationship models can be used to correct the measured gully volume and depth morphological parameter values. Because the R^2 value of the constructed gully width-to-depth ratio correction model was very low, to calculate and correct the width-to-depth ratio, the corrected gully depth can be used in place of the extracted depth data, thereby improving the accuracy of the width-to-depth ratio calculation.

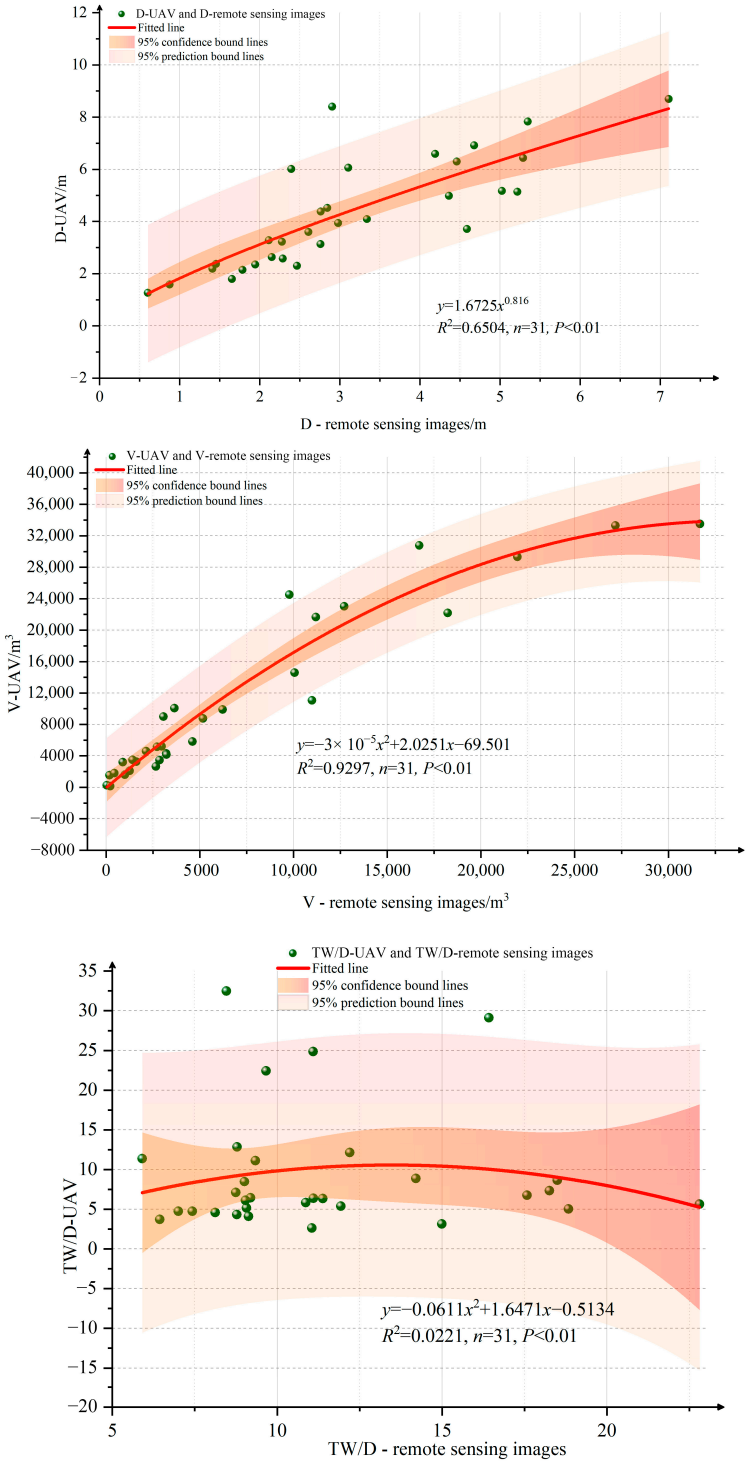

Figure 10. Three-dimensional morphology parameter regression analysis of gully extracted using the two methods.

4. Discussion

Gully erosion monitoring provides valuable data for exploring the mechanisms of gully erosion and establishing predictive models, which is particularly important for understanding the long-term evolution and erosion rates of gully systems [41]. Therefore, accurate acquisition of gully morphological parameters is required. Giménez et al. [42] analyzed the error in aerial photogrammetry (with a ground pixel size of 1.6 cm) using five sets of field measurements of gully morphology in Bardenas Reales (Navarre, Spain). They reported that the width-to-depth ratio error was small for wide and shallow gullies but was quite large and inaccurate for narrow and deep gullies. This is consistent with the results of Zhang et al. [43,44]. Castillo et al. [45] measured gully erosion morphology parameters using 3D reconstruction and lidar in Cordoba, Spain, revealing errors of less than 4% in one- and two-dimensional parameters and errors exceeding 10% in cross-sectional area. These results are consistent with the larger errors in width-to-depth ratio and gully depth reported in this study, which are mainly attributed to the increased shadow and light effects associated with narrower gullies, which are closely related to the time of photography [42]. However, in this study, the average errors in one- and two-dimensional gully morphology parameters ranged from 5 to 10%, which is very high. This is attributed to the fact that the gullies studied were mostly wide and shallow; thus, their scale is larger than that of fine and shallow gullies, resulting in relatively smaller errors.

Tang Jie et al. [18] used high-resolution (0.5 m) GeoEye-1 stereo images to extract DEMs of small watersheds in a loess hilly region and compared them with those obtained by 3D laser scanning data. They confirmed that high-resolution remote sensing stereo images can be used to measure one- and two-dimensional parameters gully parameters on loess areas. However, the measurement error of 3D parameters was relatively large, mainly concentrated within 30%. These results are consistent with our results; however, the maximum measurement error of gully depth in this study reached 50%, which is attributed to the differences in soil texture and vegetation cover in the study area. Although data collection in this study was conducted in the winter without snow to reduce the effect of vegetation cover, the presence of a small amount of fallen vegetation on the gully bottom led to larger errors in gully depth measurement [19]. Therefore, for accurate assessment of gully depth, data obtained through high-precision remote sensing methods such as actual measurements and UAV laser measurements should be used for correction.

Using high-resolution GeoEye-1 stereo images of the northern edge of the Qinghai-Tibet Plateau, Wu Jian et al. [46] showed that a single image pair can be used with only one ground control point to achieve an accuracy of 1:10,000 mapping. Li Zhen et al. [19] found that, for visual interpretation of gully morphology parameters in a loess hilly region using QuickBird images, accuracy heavily depends on the interpreter's professional knowledge and experience. Additionally, the maximum relative errors of area, perimeter, and gully length were all above 20%, but a general analysis of the total sample data showed that the errors in area, perimeter, and gully length were mainly concentrated within 10%. Our results on average error are generally consistent with Li Zhen et al.'s [19], but the maximum relative errors we reported were higher. This is attributed to wider gully mouths in our study area than in a loess hilly region, resulting in larger errors by visual interpreters (Figure 11).

This study further revealed that different visual interpreters have deviations in extracting gully mouths (Figure 11). Factors such as the spatial resolution of stereo image pairs (Figures 7 and 8), number and uniformity of ground control points in the field [11,18,46], and method of extracting DEM from stereo image pairs affect the accuracy assessment of gully morphology parameters, especially 3D ones. Nevertheless, regression models between the 3D morphology parameters gully volume and depth obtained by the two methods could be used for error correction. The error correction regression model is only applicable to this research area and cannot be guaranteed suitable for other areas owing to regional differences [17]. Gully size has various effects on the error of gully morphology parameter extraction. For example, the errors tend to increase with a decrease in gully

width, and the complexity of the gully shoulder line increases in the Loess Plateau and the typical black soil region in China [43].

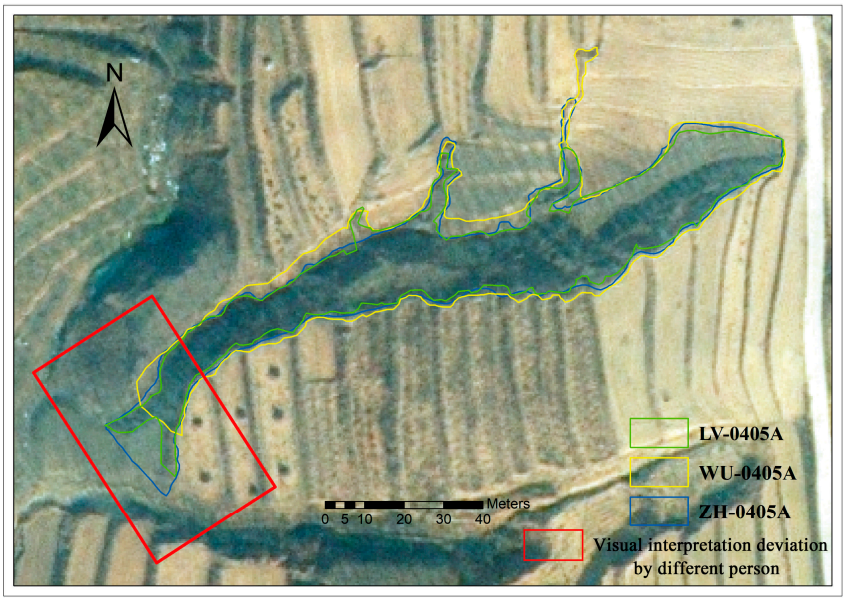

Figure 11. Deviation of the gully tail by different visual interpreters.

5. Conclusions

This study confirmed that using high-resolution remote sensing stereo image pairs to extract one- and two-dimensional parameters of gullies in a "soil-rock dual structure" area is feasible, yielding average errors of approximately 5–10%. The larger the scale of the gully, the higher the reliability of the visual interpreters in extracting 3D parameter values, resulting in smaller average relative errors. A good relationship model between the gully volume obtained from drones and high-resolution remote sensing stereo images was established and used to correct measurement biases. These findings can be applied in the monitoring and management of gully erosion in "soil–rock dual structure" areas and contribute new insights to the assessment of medium-scale soil erosion and prevention and control of soil and water loss in the region.

Author Contributions: Conceptualization, W.Z.; methodology, T.Y. and F.X.; software, F.X.; validation, S.S.; formal analysis, S.S. and T.Y.; investigation, W.Z., F.X., T.Y., W.Q., G.Z. and N.F.; resources, W.Z.; data curation, W.Z., T.Y. and F.X.; writing—original draft preparation, T.Y. and F.X.; writing—review and editing, W.Z. and S.S.; visualization, T.Y. and S.S.; supervision, W.Z.; project administration, W.Z. and W.Q.; funding acquisition, W.Z. and T.Y. All authors have read and agreed to the published version of the manuscript.

Funding: This research was funded by the National Natural Science Foundation of China (41907050, 41877073) and the Natural Science Foundation of Shandong Province (ZR2023QD030).

Data Availability Statement: The data presented in this study are available on request from the corresponding author.

Acknowledgments: The authors thank Zhikang Gao, Sizheng Wu, and Zhenghui Lv for their assistance with fieldwork.

Conflicts of Interest: The authors declare no conflicts of interest.

References

1. Poesen, J.; Nachtergaele, J.; Verstraeten, G.; Valentin, C. Gully erosion and environmental change: Importance and research needs. *Catena* **2003**, *50*, 91–133. [CrossRef]
2. Bartley, R.; Poesen, J.; Wilkinson, S.; Vanmaercke, M. A review of the magnitude and response times for sediment yield reductions following the rehabilitation of gullied landscapes. *Earth Surf. Process. Landf.* **2020**, *45*, 3250–3279. [CrossRef]

3. Anderson, R.L.; Rowntree, K.M.; Roux, J.J.L. An interrogation of research on the influence of rainfall on gully erosion. *Catena* **2021**, *206*, 105482. [CrossRef]
4. Liu, B.Z. *Soil Erosion*; Shaanxi People's Publisher: Xi'an, China, 1997; pp. 15–26. (In Chinese)
5. Majhi, A.; Nyssen, J.; Verdoodt, A. What is the best technique to estimate topographic thresholds of gully erosion? Insights from a case study on the permanent gullies of Rarh plain, India. *Geomorphology* **2021**, *375*, 107547. [CrossRef]
6. Torri, D.; Poesen, J.; Rossi, M.; Amici, V.; Spennacchi, D.; Cremer, C. Gully head modelling: A Mediterranean badland case study. *Earth Surf. Process. Landf.* **2018**, *43*, 2547–2561. [CrossRef]
7. Poesen, J. Soil erosion in the Anthropocene: Research needs. *Earth Surf. Process. Landf.* **2018**, *43*, 64–84. [CrossRef]
8. Bernatek-Jakiel, A.; Poesen, J. Subsurface erosion by soil piping: Significance and research needs. *Earth-Sci. Rev.* **2018**, *185*, 1107–1128. [CrossRef]
9. Valentin, C.; Poesen, J.; Yong, L. Gully erosion: Impacts, factors and control. *Catena* **2005**, *63*, 132–153. [CrossRef]
10. Liu, Y.B.; Zhu, X.M.; Zhou, P.H.; Tang, K.L. The laws of hillslope channel erosion occurrence and development on Loess Plateau. Memoir of NISWSC. *Acad. Sin.* **1988**, *7*, 9–18. (In Chinese)
11. Roberts, M.E.; Burrows, R.M.; Thwaites, R.N.; Hamilton, D.P. Modelling classical gullies—A review. *Geomorphology* **2022**, *407*, 108216. [CrossRef]
12. Shen, H.O.; Zheng, F.L.; Wen, L.L. A research review of rill development and morphological characteristics. *Acta Ecol. Sin.* **2018**, *38*, 6818–6825. (In Chinese)
13. Liu, G.; Zheng, F.L.; Wilson, G.V.; Xu, X.M.; Liu, C. Three decades of ephemeral gully erosion studies. *Soil Tillage Res.* **2021**, *212*, 105046. [CrossRef]
14. Zhou, X.; Wei, Y.; He, J.; Cai, C.F. Estimation of gully erosion rate and its determinants in a granite area of southeast China. *Geoderma* **2023**, *429*, 116223. [CrossRef]
15. Xiong, D.H.; Fan, J.R.; Lu, X.R.; Zhou, H.Y. A Review on the study of gully erosion. *World Sci-Tech R D* **2007**, *29*, 29–35. (In Chinese)
16. Luffman, I.E.; Nandi, A.; Spiegel, T. Gully morphology, hillslope erosion, and precipitation characteristics in the Appalachian Valley and Ridge province, southeastern USA. *Catena* **2015**, *133*, 221–232. [CrossRef]
17. Zhang, G.H.; Zhao, W.J.; Yan, T.T.; Qin, W.; Miao, X.J. Estimation of Gully Growth Rate and Erosion Amount Using UAV and Worldview-3 Images in Yimeng Mountain Area, China. *Remote Sens.* **2023**, *15*, 233. [CrossRef]
18. Tang, J.; Zhang, Y.; Fan, C.H.; Cheng, X.X.; Deng, J.Y. Accuracy assessment of gully morphological parameters from high resolution remote sensing stereoscopic satellite images on hilly Loess Plateau. *Trans. CSAE* **2017**, *33*, 111–117. (In Chinese)
19. Li, Z.; Zhang, Y.; Yang, S.; Zhu, Q.K.; Wu, J.H.; Ma, H.; He, Y.M. Error assessment of extracting morphological parameters of bank gullies by manual visual interpretation based on QuickBird imagery. *Trans. CSAE* **2014**, *30*, 179–186. (In Chinese)
20. Cui, H.; Liu, Q.J.; Zhang, H.Y.; Zhang, Y.X.; Wei, W.L.; Jiang, W.; Xu, X.L.; Liu, S.T. Long-term manure fertilization increases rill erosion resistance by improving soil aggregation and polyvalent cations. *Catena* **2023**, *223*, 106909. [CrossRef]
21. Goodwin, N.R.; Armston, J.D.; Muir, J.; Stiller, I. Monitoring gully change: A comparison of airborne and terrestrial laser scanning using a case study from Aratula, Queensland. *Geomorphology* **2017**, *282*, 195–208. [CrossRef]
22. Caraballo-Arias, N.A.; Conoscenti, C.; Di Stefano, C.; Ferro, V.; Gómez-Gutiérrez, A. Morphometric and hydraulic geometry assessment of a gully in SW Spain. *Geomorphology* **2016**, *274*, 143–151. [CrossRef]
23. Gao, C.; Li, P.; Hu, J.; Yan, L.; Latifi, H.; Yao, W.Q.; Hao, M.K.; Gao, J.J.; Dang, T.M.; Zhang, S.H. Development of gully erosion processes: A 3D investigation based on field scouring experiments and laser scanning. *Remote Sens. Environ.* **2021**, *265*, 112683. [CrossRef]
24. Feng, L.; Li, B.B. Establishment of high precision terrain model of eroded gully with UAV oblique aerial photos and ground control points. *Trans. CSAE* **2018**, *34*, 88–95. (In Chinese)
25. Li, J.J.; Xiong, D.H.; Lu, X.N.; Dong, Y.F.; Su, Z.A.; Zhai, J.; Yang, D. Morphological characteristics of the gully head in dry-hot vally based on the RTK–GPS technology. *Mt. Res.* **2014**, *32*, 706–716. (In Chinese)
26. Belayneh, M.; Yirgu, T.; Tsegaye, D. Current extent, temporal trends, and rates of gully erosion in the Gumara watershed, Northwestern Ethiopia. *Glob. Ecol. Conserv.* **2020**, *24*, e01255. [CrossRef]
27. Brecheisen, Z.S.; Richter, D.D. Gully-erosion estimation and terrain reconstruction using analyses of microtopographic roughness and LiDAR. *Catena* **2021**, *202*, 105264. [CrossRef]
28. Castillo, C.; Gómez, J.A. A century of gully erosion research: Urgency, complexity and study approaches. *Earth-Sci. Rev.* **2016**, *160*, 300–319. [CrossRef]
29. Frankl, A.; Stal, C.; Abraha, A.; Nyssen, J.; Rieke-Zapp, D.; De Wulf, A.; Poesen, J. Detailed recording of gully morphology in 3D through image-based modelling. *Catena* **2015**, *127*, 92–101. [CrossRef]
30. Ben Slimane, A.; Raclot, D.; Rebai, H.; Le Bissonnais, Y.; Planchon, O.; Bouksila, F. Combining field monitoring and aerial imagery to evaluate the role of gully erosion in a Mediterranean catchment (Tunisia). *Catena* **2018**, *170*, 73–83. [CrossRef]
31. Wang, J.X.; Zhang, Y.; Deng, J.Y.; Yu, S.W.; Zhao, Y.Y. Long-Term Gully Erosion and Its Response to Human Intervention in the Tableland Region of the Chinese Loess Plateau. *Remote Sens.* **2021**, *13*, 5053. [CrossRef]
32. Yuan, M.T.; Zhang, Y.; Zhao, Y.Y.; Deng, J.Y. Effect of rainfall gradient and vegetation restoration on gully initiation under a large-scale extreme rainfall event on the hilly Loess Plateau: A case study from the Wuding River basin, China. *Sci. Total Environ.* **2020**, *739*, 140066. [CrossRef] [PubMed]

33. le Roux, J.; Morake, L.; van der Waal, B.; Anderson, R.L.; Hedding, D.W. Intra-gully mapping of the largest documented gully network in South Africa using UAV photogrammetry: Implications for restoration strategies. *Prog. Phys. Geogr. Earth Environ.* **2022**, *46*, 772–789. [CrossRef]
34. Pineux, N.; Lisein, J.; Swerts, G.; Bielders, C.L.; Lejeune, P.; Colinet, G.; Degré, A. Can DEM time series produced by UAV be used to quantify diffuse erosion in an agricultural watershed? *Geomorphology* **2017**, *280*, 122–136. [CrossRef]
35. Song, X.P.; Zhang, Y.; Wang, Z.Q.; Deng, J.Y.; Wang, J.X. Accuracy of gully morphological parameters extracted by UAV photogrammetry in the Loess Plateau. *J. Beijing Norm. Univ. (Nat. Sci.)* **2021**, *57*, 606–612. (In Chinese)
36. Rossi, P.; Mancini, F.; Dubbini, M.; Mazzone, F.; Capra, A. Combining nadir and oblique UAV imagery to reconstruct quarry topography: Methodology and feasibility analysis. *Eur. J. Remote Sens.* **2017**, *50*, 211–221. [CrossRef]
37. Liu, K.; Ding, H.; Tang, G.A.; Na, J.M.; Huang, X.L.; Xue, Z.G.; Yang, X.; Li, F.Y. Detection of Catchment-Scale Gully-Affected Areas Using Unmanned Aerial Vehicle (UAV) on the Chinese Loess Plateau. *ISPRS Int. J. Geo-Inf.* **2016**, *5*, 238. [CrossRef]
38. Hu, F.; Gao, X.; Li, G.; Li, M. DEM Extraction from Worldview-3 Stereo-images and Accuracy Evaluation. *ISPRS Congr. Remote Sens. Spat. Inf. Sci.* **2016**, *XLI-B1*, 327–332.
39. Dong, Y.; Chen, W.; Chang, H.; Zhang, Y.; Feng, R.; Meng, L. Assessment of orthoimage and DEM derived from ZY-3 stereo image in Northeastern China. *Surv. Rev.* **2016**, *48*, 247–257. [CrossRef]
40. Li, J.J.; Liu, Q.J.; Wang, Y.; Zhang, H.Y.; Li, J.Q.; Wang, K.L.; Geng, J.B.; Wang, L.Z.; Fang, N.F. Systematic evaluation of the effects of the length, depth, and amount of incorporated maize straw on rill flow velocity. *J. Hydrol.* **2023**, *621*, 129550. [CrossRef]
41. Vanmaercke, M.; Panagos, P.; Vanwalleghem, T.; Hayas, A.; Foerster, S.; Borrelli, P.; Rossi, M.; Torri, D.; Casali, J.; Borselli, L.; et al. Measuring, modelling and managing gully erosion at large scales: A state of the art. *Earth-Sci. Rev.* **2021**, *218*, 103637. [CrossRef]
42. Giménez, R.; Marzolff, I.; Campo, M.A.; Seeger, K.M.; Alvarez-Mozos, J. Accuracy of high-resolution photogrammetric measurements of gullies with contrasting morphology. *Earth Surf. Process. Landf.* **2009**, *34*, 1915–1926. [CrossRef]
43. Zhang, C.M.; Wang, C.M.; Long, Y.Q.; Pang, G.W.; Shen, H.Z.; Wang, L.; Yang, Q.K. Comparative Analysis of Gully Morphology Extraction Suitability Using Unmanned Aerial Vehicle and Google Earth Imagery. *Remote Sens.* **2023**, *15*, 4302. [CrossRef]
44. Chen, Y.; Jiao, J.; Wei, Y.; Zhao, H.; Yu, W.; Cao, B.; Xu, H.; Yan, F.; Wu, D.; Li, H. Accuracy Assessment of the Planar Morphology of Valley Bank Gullies Extracted with High Resolution Remote Sensing Imagery on the Loess Plateau, China. *Int. J. Environ. Res. Public Health* **2019**, *16*, 369. [CrossRef] [PubMed]
45. Castillo, C.; Pérez, R.; James, M.R.; Quinton, J.N.; Taguas, E.V.; Gómez, J.A. Comparing the Accuracy of Several Field Methods for Measuring Gully Erosion. *Soil Sci. Soc. Am. J.* **2012**, *76*, 1319. [CrossRef]
46. Wu, J.; Wang, Y.W.; Liu, J.C.; Song, N.; Wang, D.Q.; Fu, J. Orientation Precision and Photogrammetry Control Point in the Plateau Area Based on Single Geo Eye-1 Image Stereopair. *Surv. Mapp.* **2020**, *43*, 220–222. (In Chinese)